Development of the ReaxFF Reactive Force Field for Describing Transition Metal Catalyzed Reactions, with Application to the Initial Stages of the Catalytic Formation of Carbon Nanotubes

Kevin D. Nielson, Adri C. T. van Duin, Jonas Oxgaard, Wei-Qiao Deng, and William A. Goddard III*

Materials and Process Simulation Center, Beckman Institute (139-74), California Institute of Technology, Pasadena, California 91125

Received: August 19, 2004; In Final Form: November 10, 2004

With the aim of developing a computationally inexpensive method for modeling the high-temperature reaction dynamics of transition metal catalyzed reactions we have developed a ReaxFF reactive force field in which the parameters are fitted to a substantial quantum mechanics (QM) training set, containing full reaction pathways for relevant reactions. In this paper we apply this approach to reactions involving carbon materials plus Co, Ni, and Cu atoms. We find that ReaxFF reproduces the QM reaction data with good accuracy while also reproducing the binding characteristics of Co, Ni, and Cu atoms to hydrocarbon fragments. To demonstrate the applicability of ReaxFF we performed high-temperature (1500 K) molecular dynamics simulations on a nonbranched all-carbon feedstock in the presence and absence of Co, Ni, and Cu atoms. We find that the presence of Co and Ni leads to substantial amounts of branched carbon atoms, leading eventually to the formation of carbon-nanotube-like species. In contrast, we find that under the same simulation conditions Cu leads to very little branching and leads to products with no nanotube character. In the absence of metals no branching is observed at all. These results suggest that Ni and Co catalyze the production of nanotube-like species whereas Cu does not. This is in excellent agreement with experimental observations, demonstrating that ReaxFF can provide a useful and computational tractable tool for studying the dynamics of transition metal catalytic chemistry.

1. Introduction

The behavior of short-lived species under extreme conditions is difficult to study via laboratory methods because of the limited information about the character of such species and the caustic conditions of the environment. Thus, it would be most useful to be able to use molecular dynamics (MD) simulations to study these species under realistic reaction conditions. In principle quantum mechanics (QM) could be used to predict the detailed behavior of such short-lived and high-energy chemical species,[1−4] but these methods are impractical to apply in most cases for the range of temperatures and time scales required to fully elucidate the mechanism and rates.

As an alternative to QM, MD simulations, employing classical force field[5−8] (FF) methods, can be used. These methods are more practical in handling the relevant time scales and range of temperatures. Unfortunately, most classical force fields (e.g., MM3,[9] Dreiding,[10] Amber[11]) with their harmonic-like bond descriptions are incapable of describing chemical reactions, while reactive empirical potentials[6,12−15] have, until recently, only been available for a limited number of chemical systems and cannot be straightforwardly transferred to other systems.

Over the last years we have been developing a branch of transferable reactive force fields (ReaxFF). Previously, we have reported ReaxFF descriptions for hydrocarbons,[16] nitramines,[17] silicon/silicon oxides,[18] and aluminum/aluminum oxides.[19] For all these materials, force field parameters were determined by fitting them to a substantial database of QM data, covering ground-state systems as well as full reactive pathways. Here we report on the development of a ReaxFF description for all-carbon materials and for the interactions between carbon and Co, Ni, and Cu, three transition metals commonly employed in catalytic transformations.

In light of previous studies on fullerene formation[3] and the nature of the carbon nanotube (CNT) growth mechanism,[4] we have employed this ReaxFF description for metal−carbon interactions to identify the characteristics that make a metal a good CNT catalyst. It is known that both Co[20,21] and Ni[22] are effective catalysts of single-walled CNT formation, whereas Cu[23,24] is much less effective. To demonstrate the validity of the ReaxFF approach for the investigation of catalytic reactions and to gain a better understanding of the properties that define a good catalyst for CNT formation we have simulated the high-temperature dynamics of reactive Co, Ni, and Cu interactions with carbon fragments (monocyclic C_{20} and acyclic C_4 fragments). We find, in good agreement with experimental observations, that both Co and Ni lead to the formation of a large number of branched carbon atoms and eventually lead to the formation of species with a clear-cut nanotube character. Cu, on the other hand, instigates only very little branching, while in the absence of a metal catalyst the carbon fragments remain exclusively linear or monocyclic.

2. Methods

QM Calculations. All metal−hydrocarbon QM calculations were performed using the hybrid DFT functional B3LYP as implemented by the Jaguar 5.0 program package.[25] This DFT functional utilizes the Becke three-parameter functional[26] (B3) combined with the correlation functional of Lee, Yang, and Par[27]

10.1021/jp046244d CCC: $30.25
Published on Web 12/31/2004

(LYP) and is known to produce good descriptions of reaction profiles for transition metal containing compounds.[28,29] The metals were described by the Wadt and Hay[30] core-valence (relativistic) effective core potential (treating the valence electrons explicitly) using the LACVP basis set with the valence double-ζ contraction of the basis functions, LACVP**. All electrons were used for all other elements using a modified variant of Pople et al.'s[31] 6-31G** basis set, where the six d functions have been reduced to five. For the all-carbon training set the QM training set was composed from DFT/B3LYP/6-31G** calculations.

ReaxFF Method. ReaxFF[16] is based on a bond order/bond distance relationship, a concept introduced by Tersoff[32] and first employed to carbon chemistry by Brenner.[6] Instantaneous bond orders (BO_{ij}'), including contributions from sigma, pi, and double-pi bonds are calculated from the interatomic distances, using eq 1; this first approximation is then corrected with overcoordination and undercoordination terms to force systems toward the proper number of bonds.

$$BO_{ij}' = BO_{ij}^{\sigma} + BO_{ij}^{\pi} + BO_{ij}^{\pi\pi} = \exp\left[p_{bo1}\left(\frac{r_{ij}}{r_0^{\sigma}}\right)^{p_{bo2}}\right] + \exp\left[p_{bo3}\left(\frac{r_{ij}}{r_0^{\pi}}\right)^{p_{bo4}}\right] + \exp\left[p_{bo5}\left(\frac{r_{ij}}{r_0^{\pi\pi}}\right)^{p_{bo6}}\right] \quad (1)$$

Equation 2 shows that ReaxFF partitions the overall system energy into contributions from various partial energy terms. These partial energies include bond energies, valence angle, lone pair, conjugation, and torsion angle terms to properly handle the nature of preferred configurations of atomic and resulting molecular orbitals and terms to handle van der Waals and Coulomb interactions. These latter nonbonded interactions are calculated between *every* atom pair, irrespective of connectivity, and are shielded to avoid excessive repulsion at short distances. This treatment of nonbonded interactions allows ReaxFF to describe covalent, ionic, and intermediate materials, thus, greatly enhancing its transferability.

$$E_{system} = E_{bond} + E_{lp} + E_{over} + E_{under} + E_{val} + E_{pen} + E_{coa} + E_{C_2} + E_{tors} + E_{conj} + E_{H-bond} + E_{vdWaals} + E_{Coulomb} \quad (2)$$

During the re-parametrization of the hydrocarbon ReaxFF description (ReaxFF^{CH}) with the QC data for all-carbon clusters we found that the energy terms described above were sufficient to capture the relative energy and geometry of most of these clusters, the only exception being the C_2 molecule. ReaxFF^{CH} erroneously predicts that the two carbons form a very strong (triple) bond, while in fact the triple bond would get de-stabilized by terminal radical electrons, and for that reason the carbon−carbon bond is not any stronger than a double bond. Because the stability of C_2 is relevant for the application described here, we introduced a new partial energy contribution (E_{C_2}). Equation 3 shows the potential function used to de-stabilize the C_2 molecule:

$$E_{C_2} = k_{c2}(BO_{ij} - \Delta_i - 0.04\Delta_i^4 - 3)^2 \quad \text{if} \quad BO_{ij} - \Delta_i - 0.04\Delta_i^4 > 3 \quad (3)$$

$$E_{C_2} = 0 \quad \text{if} \quad BO_{ij} - \Delta_i - 0.04\Delta_i^4 \le 3$$

where Δ_i is the level of under/overcoordination on atom i as obtained from subtracting the valency of the atom (4 for carbon) from the sum of the bond orders around that atom and k_{c2} is the force field parameter associated with this partial energy contribution. The factor 0.04 is chosen to ensure that the correction term only affects the C_2 molecule and has no or marginal impact on the energies of the other molecules in the training set.

TABLE 1: Relative Energies for All-Carbon Phases

compound	E_{ref} (kcal/mol)	E_{ReaxFF} (kcal/mol)
graphite	0.00	0.00
diamond	0.8	0.52
graphene	1.3	1.56
10_10 nanotube	2.8	2.83
17_0 nanotube	2.84	2.83
12_8 nanotube	2.78	2.81
16_2 nanotube	2.82	2.82
C_{60} buckyball	11.5	11.3

The parameters involved in the force field terms were tuned to the QM data using a single-parameter search optimization technique as described by van Duin et al.[33] The full set of ReaxFF equations and force field parameters have been supplied in Supporting Information.

MD Simulations. The NVT-MD simulations on $C_{20} + C_4$ mixtures were performed using a velocity Verlet approach with a time step of 0.1 fs. This relatively short time step was chosen to ensure good MD behavior at the high temperatures (1500 K) employed in our simulations. When low to moderate temperatures are used (0−1000 K) ReaxFF MD will conserve energy in NVE simulations with time steps up to 0.5 fs, and at more elevated temperatures smaller time steps need to be used to obtain good energy conservation. A Berendsen thermostat[34] with a temperature-damping constant of 250 fs was used to control the system temperature.

3. Results and Discussion

3.1. QM Calculations and Force Field Development. *All-Carbon Interactions.* To validate the ReaxFF method for the all-carbon chemistry expected to occur during nanotube formation, a number of relevant cases were added to the original hydrocarbon training set, after which the force field parameters were reevaluated to optimize the reproduction of both the hydrocarbon and the all-carbon data. In the original hydrocarbon training set we already included graphite, diamond, and buckyball crystals; to these crystal cases we added the relative stabilities of a number of nanotubes and compared the ReaxFF calculated stability of these systems with the results obtained from the nonreactive graphite force field of Guo et al.[35] Table 1 shows the ReaxFF results for the all-carbon phases in the training set.

The data in Table 1 indicate that ReaxFF gives a good nonreactive description of these stable all-carbon phases. To obtain a valid description of potential intermediates in nanotube formation, however, we also have to test the ReaxFF energies for smaller all-carbon fragments. To perform this test, we performed QM simulations on a number of these fragments and tested the ReaxFF description against these relative stabilities. Figure 1 shows the comparison between the ReaxFF and the DFT results.

The results in Figure 1 demonstrate that ReaxFF gives a good description of the relative energies for the all-carbon fragments. In accordance with the DFT data, ReaxFF predicts that for fragments smaller than C_{10} the linear form is the most stable configuration, while polycyclic structures become energetically favorable for structures with 20 carbon atoms or more. ReaxFF reproduces the strain in three-membered ring species, which are likely to be important intermediates in all-carbon reactions.

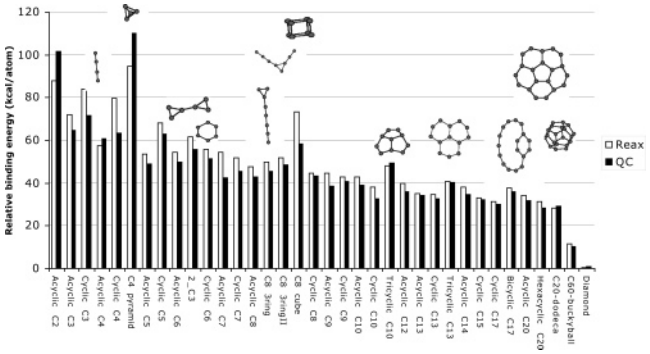

Figure 1. DFT and ReaxFF^C relative stabilities for small all-carbon fragments.

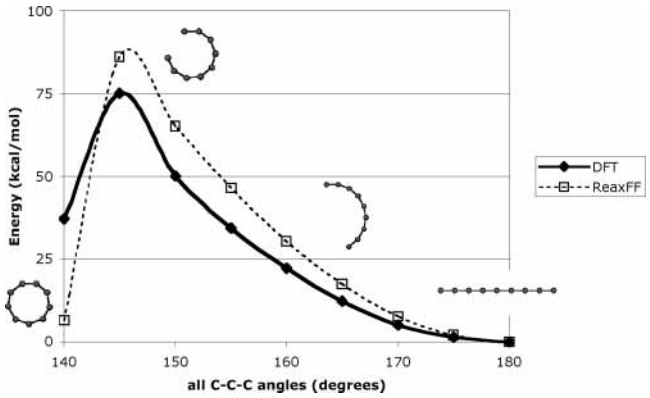

Figure 2. DFT and ReaxFF energy profiles for the cyclization reaction in C_9. This reaction profile was obtained by constraining all C−C−C angles.

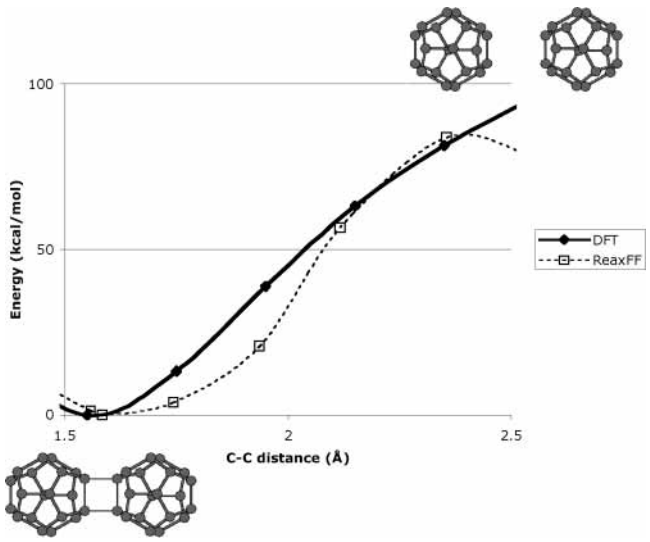

Figure 3. DFT and ReaxFF energy profiles for the coalescence reaction between two C_{20} dodecahedrons.

Table 1 and Figure 1 establish the ReaxFF credentials as a nonreactive force field for all-carbon materials; Figures 2−4 demonstrate how ReaxFF performs when tested against DFT data describing reactive events.

The results in Figure 2 demonstrate that ReaxFF can describe angle bending in all-carbon compounds, even beyond the reactive limit, while the results in Figures 3 and 4 show that ReaxFF can describe the formation and dissociation of chemical bonds in complicated configurations. As mentioned, all the reactive and nonreactive data in the hydrocarbon training set (including dissociation of single, double, and triple bonds, radical rearrangement reactions, reactions including conjugated systems,

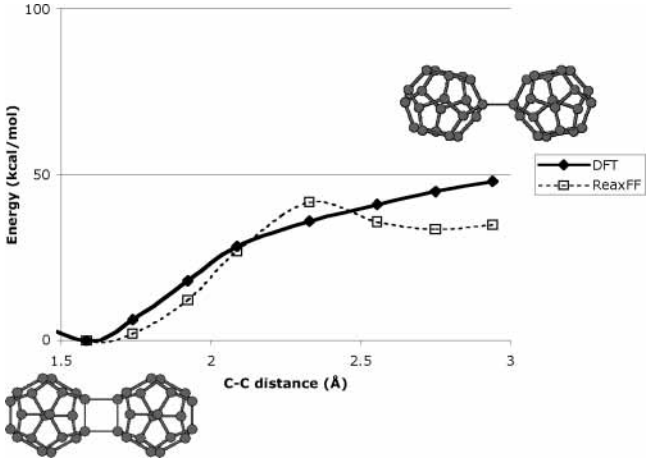

Figure 4. DFT and ReaxFF energy profiles for the dissociation of one bond between two coalesced C_{20} dodecahedrons.

and Diels−Alder, methyl-, and hydrogen-shift reactions) were used in addition to these all-carbon data to train the ReaxFF parameters. The results for these hydrocarbon cases are comparable or better than those reported earlier.[16] As such, we believe that ReaxFF should provide a reliable, computationally inexpensive method for simulating reactive events in all-carbon materials.

Metal−Carbon Interactions. Important structures (depicted in Figure 5) were identified, constructed, and optimized to give ground-state structures. Dissociation profiles of these structures were then constructed, constraining a bond length or angle of choice over a range both below and above the equilibrium value. Furthermore, by calculating the energies on reactants and reaction products separately key bond dissociation energies were determined (Table 2).

Structures were selected so that a rigorous, quantum chemical description would exist for geometrically significant or common atomic arrangements while still limiting the number of calculations to be performed. We believed it to be important to characterize a metal's ability to singly bind one, two, or three carbons because this occurs very frequently and indicates the ability to achieve high coordination states, a strongly differentiating characteristic among catalysts. Also important to this characteristic is the freedom for bond angle bending about the metal, indicating the ease with which new carbon atoms can be coordinated. The behavior of doubly bound carbon is important because of the role it plays in ring formation, of key interest in many catalysis problems.

The behavior of metals around rings and proto-rings is also an important descriptor. To this end, the behavior of metals in five- and six-membered metallocycles (four- and five-C chains) is important because it determines the rate at which a catalyst can enter or leave these formations, indicating the relative rate of small ring expansion. Upon formation of stable six-membered rings, the most likely role of a metal is as part of a benzyne complex. Also important is the dissociation of a metal from an aromatic six-membered ring, as in benzene, with a dissociation path parallel to the axis of the π system.

Structures were constructed so as to provide as simple an electronic arrangement as possible. For Co and Cu cases, singlet states were frequently constructed through the addition of a methyl group as compared to the Ni cases. This allowed for more accurate energy determination and decreased computational expense. Also, hydrocarbon frameworks were used instead of all-carbon frameworks so as to clearly define the lowest energy spin state of the system.

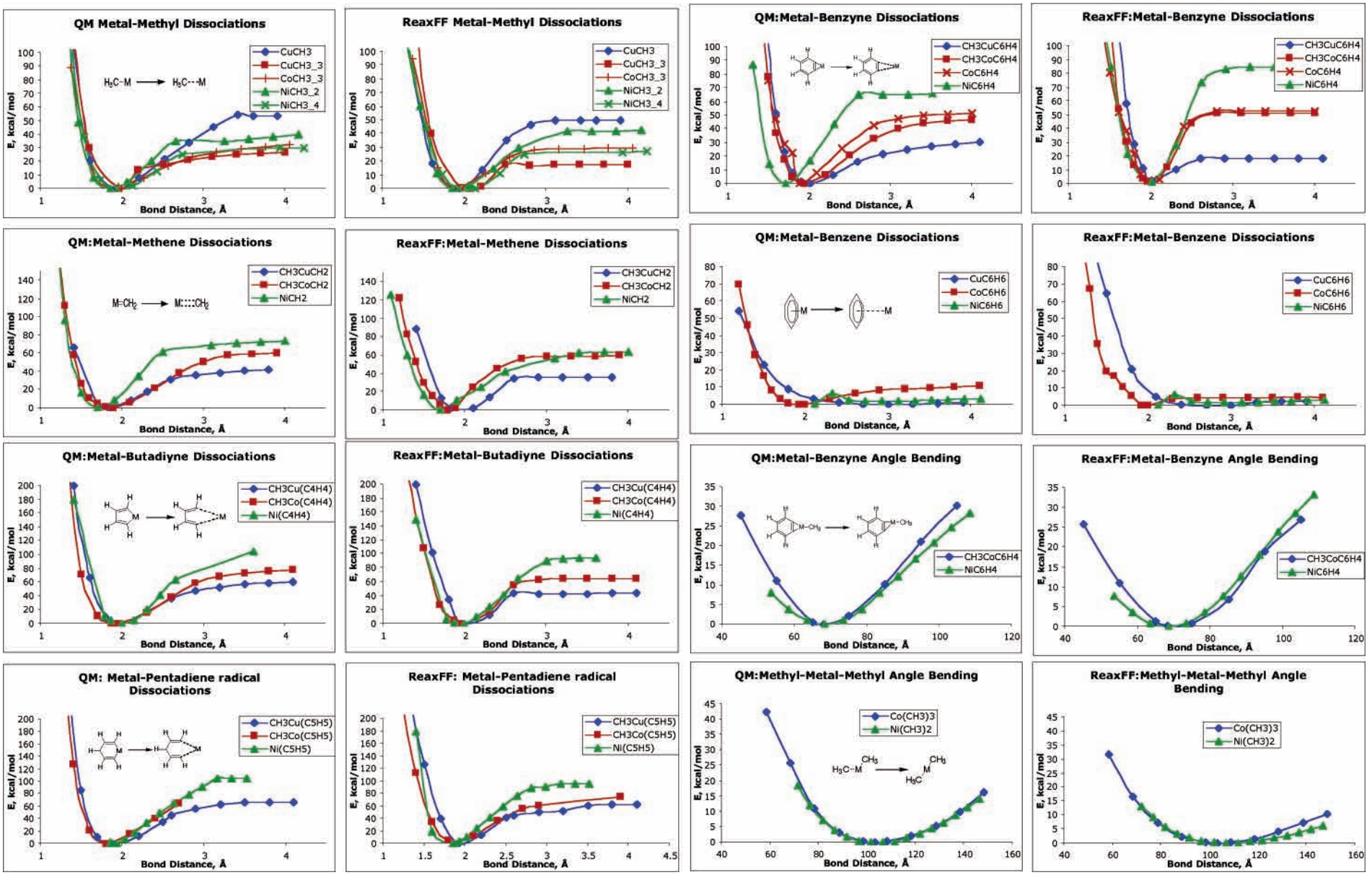

Figure 5. QM and ReaxFF data for bond dissociations and angle distortion in metal/hydrocarbon complexes.

TABLE 2: Bond Dissociation Energies (in kcal/mol) Used in Parameterizing the Force Field

reactant	products	E_{diss}(QM)	E_{diss}(ReaxFF)
$CuCH_3$	$Cu + CH_3$	54.2	50.3
$Cu(CH_3)_2$	$CH_3Cu + CH_3$	26.4	30.2
$Cu(CH_3)_3$	$(CH_3)_2Cu + CH_3$	28.2	16.5
$CH_3Cu{=}CH_2$	$CH_3Cu + CH_2$	44.8	36.1
Cu−benzene	Cu + benzene	2.50	2.5
$CoCH_3$	$Co + CH_3$	53.3	42.6
$Co(CH_3)_2$	$CH_3Co + CH_3$	37.4	38.4
$CH_3Co{=}CH_2$	$CH_3Co + CH_2$	60.8	59.5
Co−benzene	Co + benzene	3.1	4.2
$Ni(CH_3)_2$	$NiCH_3 + CH_3$	39.5	42.4
$Ni(CH_3)_4$	$Ni(CH_3)_3 + CH_3$	30.2	27.6
$Ni{=}CH_2$	$Ni + CH_2$	76.0	64.1
Ni−benzene	Ni + benzene	2.5	2.9

For cases making a spin state transition during dissociation, dissociation curves for both spin states were calculated. The lowest of the two is assumed to be the natural dissociation path. These data represent the important options for interactions between the carbon and the metal atoms and were used to calibrate the force field. For each case, good agreement between the QM data and the ReaxFF energies is observed (Figure 5, Table 2).

In addition to the parametrization of ReaxFF, a number of important observations can be made from these data. Both Co and Ni readily form multiple bonds (≥ 3) necessary for creating new C−C bonds, and bond angles are flexible ($\pm 25°$ at a cost of ~5 kcal/mol) allowing coordination of additional carbons. Cu coordinates a single carbon very tightly (~54 kcal/mol) but accepts secondary and tertiary carbons very reluctantly (only 28 and 26 kcal/mol, respectively), indicating a tendency to remain inactive under conditions where Co and Ni would likely be active, thus, indicating that Cu may fail to catalyze small ring formation.

Co, Cu, and Ni all dissociate readily from benzene rings (binding energy ~3 kcal/mol), allowing them to catalyze the formation of highly stable rings and subsequently depart for further catalysis. Both Co and Ni bind well to five-membered rings (~65 kcal/mol and ~125 kcal/mol, respectively), making it unlikely that the ring will close on its own before having another carbon introduced to form a six-membered ring.

In benzyne complexes, both Co and Ni bind well to benzyne (~40 kcal/mol and ~60 kcal/mol, respectively) allowing them to play a role in extending graphitic sheets. Cu binds weakly in this situation (~30 kcal/mol), suggesting that it cannot function to extend graphitic sheets. For Co and Ni cases, small changes in the bond angle are energetically inexpensive, allowing new carbons to bind to the benzyne, displacing the metal and extending the graphitic sheet.

3.2. Application of ReaxFF to the Initial Stages of Metal Catalyzed Nanotube Formation. To test the validity of the ReaxFF method for studying metal catalyzed nanotube growth, we performed NVT-MD simulations at a temperature of 1500 K on a 20 × 20 × 20 Å periodic box containing 5 C_{20} monocyclic rings and 10 C_4 acyclic chains. This initial configuration was chosen in accordance with earlier mechanistic studies that indicate that nanotube growth initiates from monocyclic carbon rings.[36,37] To test the impact of metal catalysts on this system and to differentiate between the relative capability of Cu, Ni, and Co to catalyze nanotube growth these simulations were performed without metal atoms and with 15 Cu, Ni, or Co atoms added (Figure 6). To avoid formation of metal clusters, which might lower the catalytic ability of the metals, we lowered the metal−metal bond dissociation parameters to 0.0 kcal/mol.

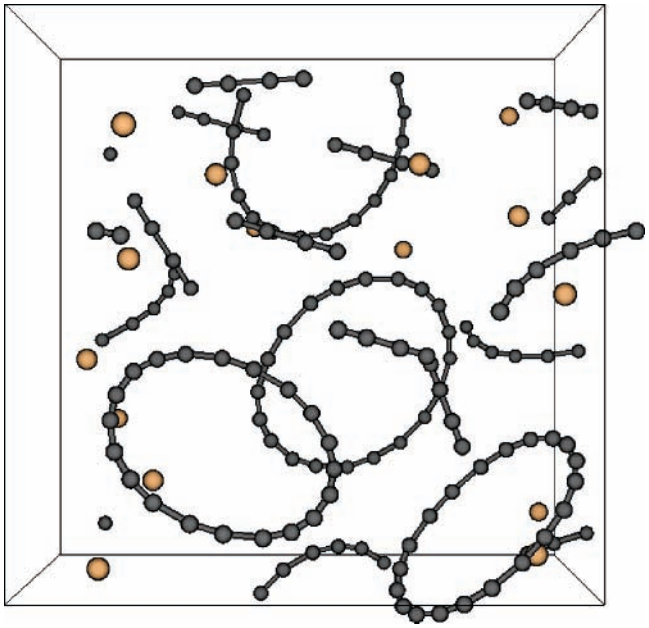

Figure 6. Initial configuration, involving 5 C_{20} monocyclic rings, 10 C_4 acyclic chains, and 15 Cu atoms, employed in the NVT-MD simulations.

TABLE 3: Number of Branched and Unbranched Carbon Atoms Observed in the 90-ps Configuration of the NVT-MD Simulations[a]

system description	number of unbranched carbons	number of branched carbons
no metal	140	0
Cu	137	3
Co	104	36
Ni	85	55

[a] A branched carbon is defined as a carbon involved in three or more bonds, each with a bond order greater than 0.3, to other carbon atoms; an unbranched carbon has one or two bonds.

These conditions were chosen to maximize the possible effect of metal catalysis, thus, to increase the odds of differentiating between the various transition metals, and were not aiming to directly reflect realistic nanotube growth conditions. More realistic growth conditions, involving a more diverse carbon feedstock and a lower metal concentration, thus, requiring larger systems and longer simulations due to reduced metal−carbon reaction rates, will be the subject of future studies.

As Figure 7 and Table 3 demonstrate, we did not observe any meaningful steps toward nanotube formation in the absence of metal atoms; the C_4 acyclic chains polymerized and some of the C_{20} rings opened but no branching (as defined by carbon atoms with three or more strongly bound neighbors) was observed. Although nanotube formation would eventually be exothermic, the energy barriers for the initial branching steps seem too high to be observable on the time scales of our simulations without addition of a catalyst. In the presence of transition metal catalysts, however, we do see a significant amount of branching occurring in our simulations, leading, especially in the Ni case, to the formation of small polycyclic structures (Figure 7c) that provide nucleation points for the formation of nanotube-like structures after prolonged simulations (Figure 8). Furthermore, our data suggest that Ni and Co are far more capable of initiating carbon branching than Cu, which is in good agreement with experimental observations. These results demonstrate that ReaxFF provides a computationally inexpensive method to establish the catalytic potential of

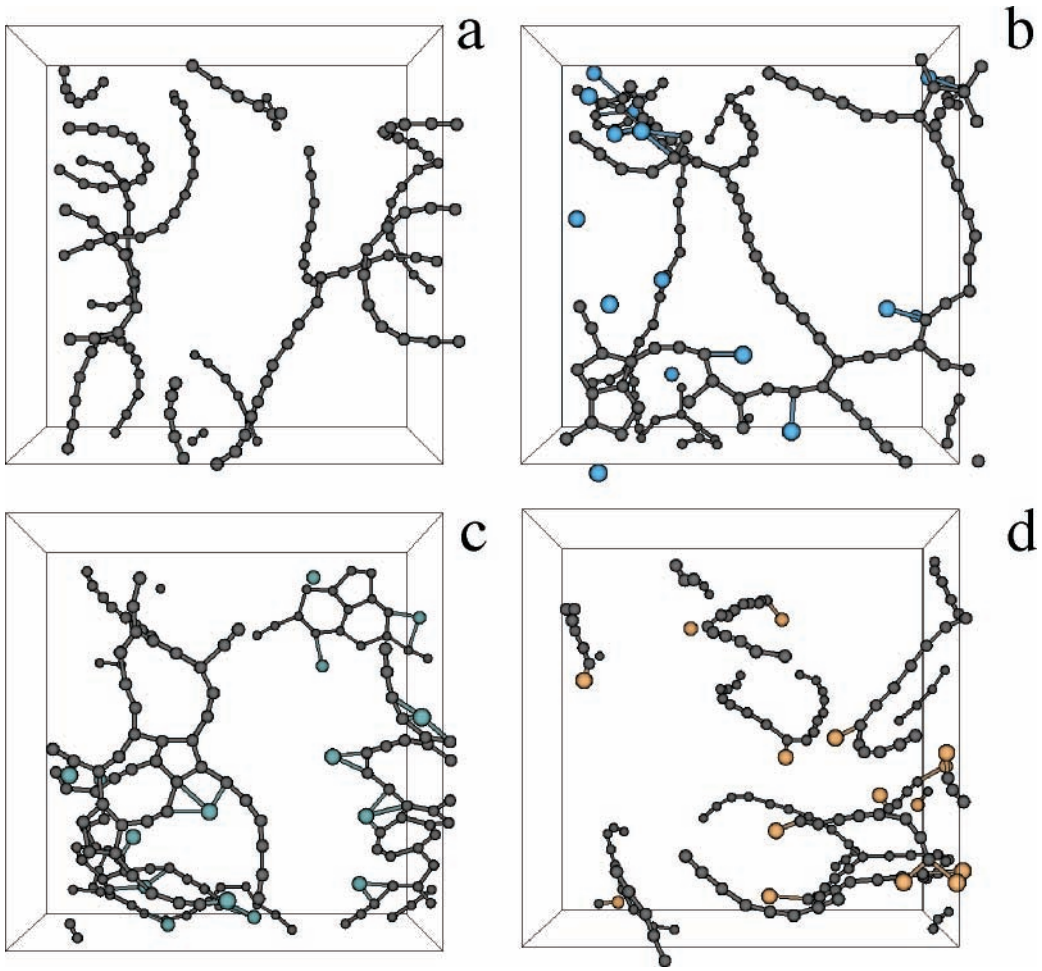

Figure 7. Configurations obtained after 90 ps of NVT-MD simulation without metal (a) and with 15 Co (b), Ni (c), and Cu (d).

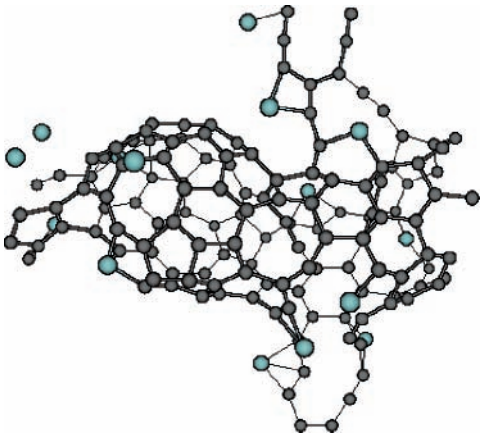

Figure 8. Configuration obtained from the NVT-MD simulation with 15 Ni atoms after 750 ps.

transition metals by allowing fully dynamical reactive simulations on complicated chemical systems.

4. Conclusions

Using the ReaxFF strategy of combining a generic form of a force field suitable for describing reactive processes with data from a substantial QM training set, including full pathways for relevant reactions, we managed to develop a reactive force field for hydrocarbons, all-carbon materials, and Cu−, Co−, and Ni−carbon interactions. We applied ReaxFF to the study the activity of Cu, Co, and Ni metal atoms for initiating nanotube growth. We find that, during high-temperature (1500 K) NVT-MD simulations in the presence of Co and Ni, substantial amounts of branched carbon atoms are formed from a linear and monocyclic all-carbon feedstock. This leads to the formation of small polycyclic structures that serve as nucleation points for further nanostructure formation. In contrast to Ni and Co, we find that Cu barely instigates branching, while in the absence of a metal catalyst no branching is observed at all. These findings are in good agreement with experimental observations, indicating that reactive force fields, if properly parametrized against a relevant QM-derived training set, can provide a useful tool for studying transition metal catalytic processes.

Acknowledgment. K.D.N. thanks NSF-CSEM for a MURF-summer fellowship. This research was supported partially by NSF-NIRT and MARCO-FENA. The computation facilities of the MSC have been supported by grants from ARO-DURIP, ONR-DURIP, NSF (MRI, CHE), and IBM-SUR. In addition the MSC is supported by grants from DoE ASCI, ARO-MURI, ARO-DARPA, ONR-MURI, NIH, ONR, General Motors, ChevronTexaco, Seiko-Epson, Beckman Institute, and Asahi Kasei. We thank the reviewers for their useful comments on this manuscript.

Supporting Information Available: A document containing the full ReaxFF potential functions and an ASCI-text file with the force field parameters described in this manuscript (readable by the ReaxFF program). This material is available free of charge via the Internet at http://pubs.acs.org.

References and Notes

(1) Car, R.; Parrinello, M. *Phys. Rev. Lett.* **1985**, *55*, 2471.
(2) Irle, S.; Zheng, G.; Elstner, M.; Morokuma, K. *Nano Lett.* **2003**, *3*, 465.
(3) Irle, S.; Zheng, G.; Elstner, M.; Morokuma, K. *Nano Lett*. **2003**, *3*, 1657.
(4) Mann, D. J.; Halls, M. D.; Hase, W. L. *J. Phys. Chem. B* **2002**, *106*, 12418.
(5) Elert, M. L.; Zybin, S. V.; White, C. T. *J. Chem. Phys*. **2003**, *118*, 9795.
(6) Brenner, D. W. *Phys. Rev. B* **1990**, *42*, 9458.
(7) Borodin, O.; Smith, G. D.; Bedrov, D. *J. Phys. Chem. B* **2002**, *106*, 9912.
(8) Canongia Lopes, J. N.; Deschamps, J.; Padua, A. A. H. *J. Phys. Chem. B* **2004**, *108*, 2038.
(9) Allinger, N. L.; Yuh, Y. H.; Lii, J.-H. *J. Am. Chem. Soc*. **1989**, *111*, 8551.
(10) Mayo, S. L.; Olafson, B. D.; Goddard, W. A. *J. Phys. Chem.* **1990**, *94*, 8897.
(11) Cornell, W. D.; Cieplak, P.; Bayly, C.; Gould, I. R.; Merz, K. M.; Ferguson, D. M.; Spellmeyer, D. C.; Fox, T.; Caldwell, J. W.; Kollman, P. A. *J. Am. Chem. Soc*. **1995**, *117*, 5179.
(12) Marks, N. A. *Phys. Rev. B* **2000**, *63*, 035401.
(13) Stuart, S. J.; Tutein, A. B.; Harrison, J. A. *J. Chem. Phys.* **2000**, *112*, 6472.
(14) Brenner, D. W.; Shenderova, O. A.; Harrison, J. A.; Stuart, S. J.; Ni, B.; Sinnott, S. B. *J. Phys.: Condens. Matter* **2002**, *14*, 783.
(15) Los, J. H.; Fasolino, A. *Phys. Rev. B* **2003**, *68*, 024107.
(16) van Duin, A. C. T.; Dasgupta, S.; Lorant, F.; Goddard, W. A. *J. Phys. Chem. A* **2001**, *105*, 9396.
(17) Strachan, A.; van Duin, A. C. T.; Chakraborty, D.; Dasgupta, S.; Goddard, W. A. *Phys. Rev. Lett.* **2003**, *91*, 098301.
(18) van Duin, A. C. T.; Strachan, A.; Stewman, S.; Zhang, Q.; Xu, X.; Goddard, W. A. *J. Phys. Chem. A* **2003**, *107*, 3083.
(19) Zhang, Q.; Cagin, T.; van Duin, A. C. T.; Goddard, W. A.; Qi, Y.; Hector, L. G. *Phys. Rev. B* **2004**, *69*, 045423.
(20) Kiang, C. H.; Goddard, W. A., III; Beyers, R.; Salem, J. R.; Bethune, D. S. *J. Phys. Chem*. **1994**, *98*, 6612.
(21) Kiang, C. H. *J. Phys. Chem. A* **2000**, *104*, 2454.
(22) Vander Wal, R. L.; Ticich, T. M. *J. Phys. Chem. B* **2001**, *105*, 10249.
(23) Vander Wal, R. L.; Ticich, T. M.; Curtis, V. E. *Carbon* **2001**, *39*, 2277.
(24) Luo, G. H.; Li, Z. F.; Wei, F.; Deng, X. Y.; Yong, J. *Physica B* **2002**, *323*, 314.
(25) *Jaguar 5.0*; Schrodinger, Inc.: Portland, Oregon, 2000.
(26) Becke, A. D. *J. Chem. Phys.* **1993**, *98*, 5648.
(27) Lee, C.; Yang, W.; Parr, R. G. *Phys. Rev. B* **1988**, *37*, 785.
(28) Baker, J.; Muir, M.; Andzelm, J.; Scheiner, A. In *Chemical Applications of Density-Functional Theory*; Laird, B. B., Ross, R. B., Ziegler, T., Eds.; ACS Symposium Series 629; American Chemical Society: Washington, DC, 1996.
(29) Niu, S.; Hall, B. M. *Chem. Rev.* **2000**, *100*, 353.
(30) (a) Hay, P. J.; Wadt, W. R. *J. Chem. Phys.* **1985**, *82*, 299. (b) Goddard, W. A., III. *Phys. Rev.* **1968**, *174*, 659. (c) Melius, C. F.; Olafson, B. O.; Goddard, W. A., III. *Chem. Phys. Lett.* **1974**, *28*, 457.
(31) (a) Hariharan, P. C.; Pople, J. A. *Chem. Phys. Lett.* **1972**, *16*, 217. (b) Francl, M. M.; Pietro, W. J.; Hehre, W. J.; Binkley, J. S.; Gordon, M. S.; DeFrees, D. J.; Pople, J. A. *J. Chem. Phys.* **1982**, *77*, 3654.
(32) Tersoff, *J. Phys. Rev. B* **1988**, *37*, 6991.
(33) van Duin, A. C. T.; Baas, J. M. A.; van de Graaf, B. *J. Chem. Soc., Faraday Trans.* **1994**, *90*, 2881.
(34) Berendsen, H. J. C.; Postma, J. P. M.; van Gunsteren, W. F.; DiNola, A.; Haak, J. R. *J. Chem. Phys.* **1984**, *81*, 3684.
(35) Guo, Y.; Karasawa, N.; Goddard, W. A. *Nature* **1991**, *351*, 464.
(36) Kiang, C. H.; Goddard, W. A. *Phys. Rev. Lett.* **1996**, *76*, 2515.
(37) Deng, W. Q.; Xu, X.; Goddard, W. A. *Nano Lett.* **2004**, *4*, 2331.